Science Advances
AAAS

Supplementary Materials for

Loss of ATF4 leads to functional aging-like attrition of adult hematopoietic stem cells

Yan Sun*, Xiaolin Lin, Bangdong Liu, Yaxuan Zhang, Wei Li, Sheng Zhang, Falian He, Han Tian, Xun Zhu, Ximeng Liu, Jueheng Wu, Junchao Cai*, Mengfeng Li*

*Corresponding author. Email: limf@mail.sysu.edu.cn (M.L.); suny69@mail.sysu.edu.cn (Y.S.); caijch3@mail.sysu.edu.cn (J.C.)

Published 22 December 2021, *Sci. Adv.* **7**, eabj6877 (2021)
DOI: 10.1126/sciadv.abj6877

This PDF file includes:

Supplementary Tables

Table S1 Technical specifications of the antibodies (clones and sources) employed in flow cytometry analysis

Antigen/Specificity	Conjugation	Host	Clone	Source	Cat. No
mouse CD16/32	PE	Rat	93	Biolegend	101307
mouse CD127 (IL-7Rα)	Biotin	Rat	A7R34	Biolegend	135005
mouse CD48	FITC	Armenian Hamster	HM48-1	Biolegend	103403
mouse/human CD11b	PE	Rat	M1/70	Biolegend	101208
mouse CD3e	APC	Armenian Hamster	145-2C11	Biolegend	100312
mouse/human CD11b	APC	Rat	M1/70	Biolegend	101212
mouse/human CD45R/B220	APC	Rat	RA3-6B2	Biolegend	103212
mouse Ly-6G/Ly-6C (Gr-1)	APC	Rat	RB6-8C5	Biolegend	108412
mouse Ly-6A/E (Sca-1)	Pacific Blue™	Rat	D7	Biolegend	108120
mouse CD117 (c-kit) 2B8	PE/Cy7	Rat	2B8	Biolegend	105814
mouse CD45.1	Alexa Fluor® 700	Mouse	A20	Biolegend	110724
mouse CD45.1	PE	Mouse	A20	Biolegend	110708
mouse CD45.2	FITC	Mouse	104	Biolegend	109806
mouse CD150 (SLAM)	APC	Rat	TC15-12F12.2	Biolegend	115910
mouse CD150 (SLAM)	Alexa Fluor® 647	Rat	TC15-12F12.2	Biolegend	115918
streptavidin	APC/Cy7	Rat		Biolegend	405208
mouse CD3e	Alexa Fluor® 647	Armenian Hamster	145-2C11	Biolegend	100322
mouse/human CD11b	Alexa Fluor® 647	Rat	M1/70	Biolegend	101218
mouse CD34	FITC	Rat	RAM34	eBioscience	11-0341-82
mouse Ly-6A/E (Sca-1)	PE	Rat	D7	eBioscience	12-5981-82
human/mouse HIF-1 alpha phycoerythrin MAb	PE	Mouse	241812	R&D	MAB1935
mouse IgG1 phycoerythrin isotype control	PE	Mouse	11711	R&D	IC002P

Table S2 Primers used in quantitative real-time PCR assay

Gene	Forward primer (5'-3')	Reverse primer (5'-3')
HIF1α	CTGTCTGCCACTTTGAATCAAAGAAATACTG	GGTTGCTGCAATAATGTTCCAATTCCTG
HIF1α	ACCTTCATCGGAAACTCCAAAG	CTGTTAGGCTGGGAAAAGTTAGG
P16	CTGGGTGCTCTTTGTGTTCC	TGCTTGAGCTGAAGCTATGC
GAPDH	AGAAGACTGTGGATGGCCCCTC	GATGACCTTGCCCACAGCCTT

Table S3 Primers used for genotyping of *ATF4$^{fl/fl}$* and *ATF4$^{fl/fl}$; Scl-Cre-ERT* mice

NO.	primer name	Sequence
1	707389-*Atf4*-dsDNA-5wt-tF1（1）	TTGGCCGTATTAGGACGCGA
	707389-*Atf4*-dsDNA-5wt-tR1（1）	ACAGCAACACTGCTGCTGGA
2	707389-*Atf4*-ssDNA-D5-5tF1（3）	GCCTAAGCCATGGCGTGAGT
	LAR3（3）	CACAACGGGTTCTTCTGTTAGTCC
3	707389-*Atf4*-ssDNA-D3-5tF1（5）	ATGTAGGCAGGAAGCTGGGA
	common_*En2*-R（5）	CCAACTGACCTTGGGCAAGAACAT
4	*Scl-Cre*-F	TCGATGCAACGAGTGATGAG
	Scl-Cre-R	TCCATGAGTGAACGAACCTG
5	*Myo*-F	TTACGTCCATCGTGGACAGC
	Myo-R	TGGGCTGGGTGTTAGCCTTA

Table S4 List of antibodies and suppliers used in the study

Antigen/Specificity	Host	Clone	Source	Cat. No	Application
ATF4	Rabbit	EPR18111	Abcam	ab184909	ChIP assay
CDKN2A/p16^{Ink4a}	Rabbit		Abcam	ab189034	WB
beta-actin	Rabbit	AG14521	Proteintech	20536-1-AP	WB

Supplementary information

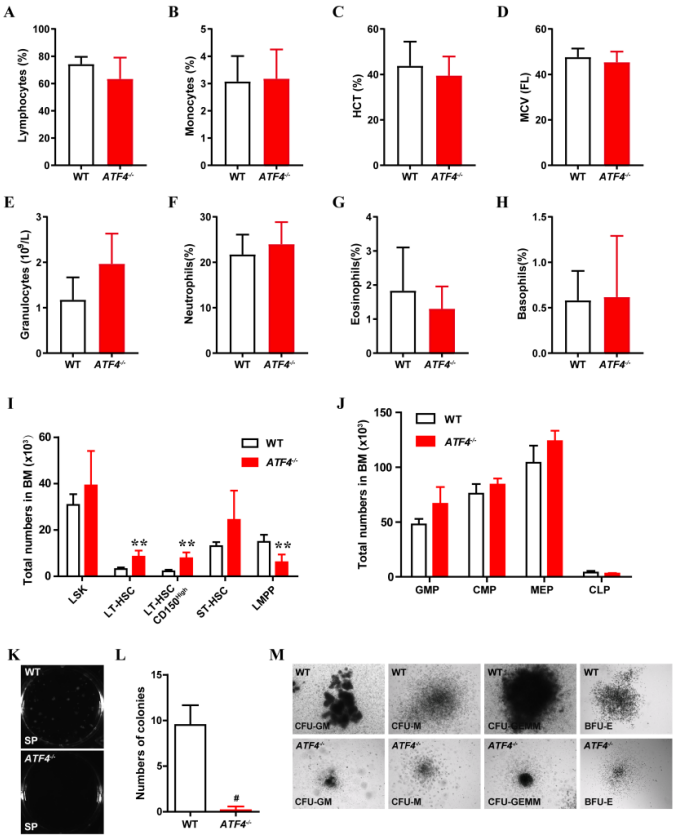

fig. S1. ATF4 is essential for the homeostasis of HSPCs in adult BM.

(A-H) Peripheral blood cell counts of WT mice and *ATF4*$^{-/-}$ mice (4 months). Peripheral blood collected from the postorbital vein was analyzed using a blood cell counter (n=3-7 per group). HCT: hematocrit; MCV: mean cell volume.

(I, J) The total numbers of LSK cells, LT-HSCs, ST-HSCs, LMPPs and CD150^{high}-HSCs (**I**), and GMPs, CMPs, MEPs and CLPs (**J**) in BM cells of WT mice and *ATF4*$^{-/-}$ mice (2-4 months) (n =3-4 mice per group).

(K-M) In vitro colony-forming unit-spleen (CFU-S) assays.

(K, L) Representative images of total CFU colonies (**K**) and graph (**L**) show quantification of changes in the total numbers of CFU colonies derived from spleen cells of *ATF4*$^{-/-}$ and WT mice (n=6).

(**M**) Representative images of hematopoietic progenitor cell colonies from spleen cells of *ATF4*$^{-/-}$ and WT mice.

**P*<0.05, ***P*<0.01 and $^{\#}$*P*<0.001 (t test).

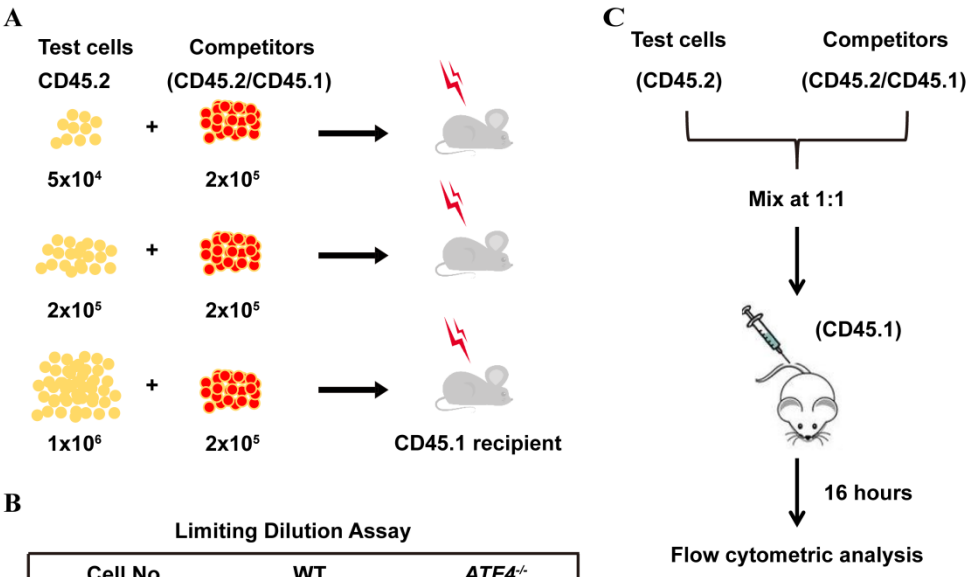

B

Limiting Dilution Assay

Cell No.	WT	*ATF4*$^{-/-}$
50K	7/8	0/8
200K	7/7	5/8
1000K	7/7	7/8
CRU Frequency / 1x10^{7} BM cells	174	13
P value	4.13x10E-7	

fig. S2. Deletion of ATF4 impairs the function of HSCs.

(A) Illustration of limiting dilution assay (LDA) procedure.

(B) Table shows the dose of donor cells and recipient mice for the LDA, and the HSC frequency in BM cells of *ATF4*$^{-/-}$ and WT mice (n=7-8 mice per group).

(C) Schematic illustration of homing assay.

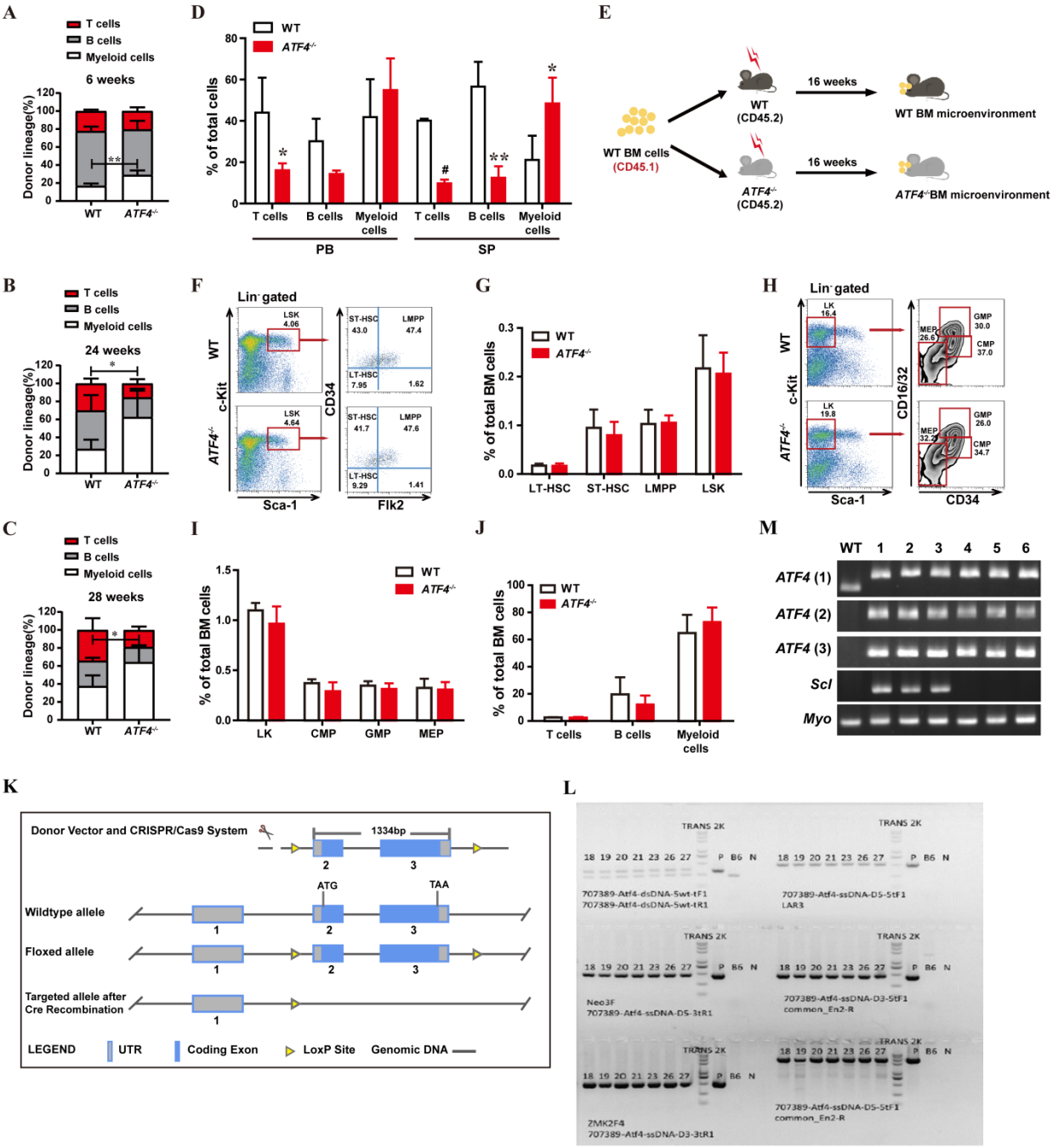

fig. S3. ATF4 deficiency provokes HSC impairment via cell-intrinsic mechanisms.

(A-C) Graphs displaying the percentages of donor-derived T, B and myeloid cells in recipient PB at 6, 24 and 28 weeks after BMT (n=2-5 mice per group).

(D) Bar graphs display the percentages of the donor-derived T, B and myeloid cells in PB and spleens of WT recipients (n=2-4 mice per group).

(E) Illustration of reciprocal BMT procedure.

(F, G) Representative FACS plots (**F**) and histograms (**G**) showing the frequencies of donor-derived

LSK cells, LT-HSCs, ST-HSCs and LMPPs in total BM cells from WT and *ATF4*$^{-/-}$ recipients (n =5-6 mice per group).

(H, I) Representative FACS plots (**H**), and histograms (**I**) showing the frequencies of donor-derived GMPs, CMPs, MEPs and LKs in total BM cells from WT and *ATF4*$^{-/-}$ recipients (n=3 mice per group).

(J) Frequencies of donor-derived T, B and myeloid cells in total BM cells from WT and *ATF4*$^{-/-}$ recipients (n=3 mice per group).

(K-M) Establish and identification of *ATF4* conditional knockout (cKO) mice (NBRI).

(**K**) Project description.

1. Transcript *Atf4*-201(ENSMUST00000109605.3) selected for presentation of the recommended strategy.

2. *Atf4*-201 gene has 3 exons, with the ATG start codon in exon 2 and TAA stop codon in exon 3.

3. Construct *Atf4* conditional knockout mice via CRISPR/Cas9 system. Cas9 mRNA, sgRNA and donor will co-injected into zygotes. sgRNA direct Cas9 endonuclease cleavage in intron 1-2 and downstream of exon 3, and create a DSB (double-strand break). Such breaks will be repaired, and result in loxP sites inserted into intron 1-2 and downstream of exon 3 respectively by homologous recombination. When mating with Cre expression allele, sequence between two loxP sites deleted in specific tissues or cells, so *Atf4* gene will disrupted.

4. The pups will be genotyped by PCR, followed by sequence analysis.

5. KO allele obtained after Cre-mediated recombination.

(**L**) Note: B6: negative control of which template is genomic DNA of C57BL/6J mice.

N: blank control without template.

TRANS 2K marker size: 2000bp, 1000bp, 750bp, 500bp, 250bp, 100bp

Analysis and conclusion: Fl/wt: 18#-21#，23#，26#，27#.

(**M**) Identification of the F1 generation of *Atf4* cKO mice (NBRI)

**P*<0.05, ***P*<0.01 and $^{\#}$*P*<0.001 (t test).

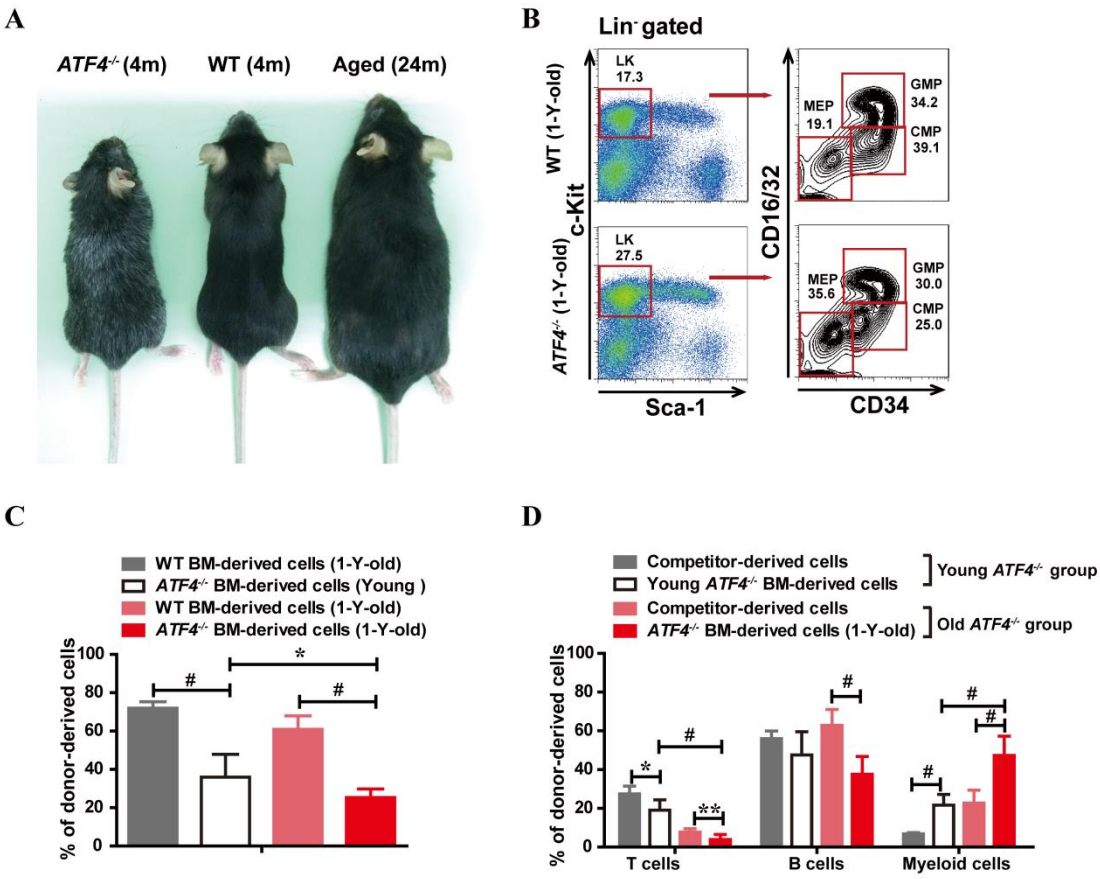

fig. S4. ATF4 deficiency leads to HSC defects with an aging-like phenotype.

(A) Representative images of WT mice, *ATF4*$^{-/-}$ mice and aged mice.

(B) Representative FACS plots of GMPs, CMPs and MEPs in BM cells from WT mice (1-year-old) and *ATF4*$^{-/-}$ mice (1-year-old).

(C) Recipient mice were analyzed for the contribution of WT (1-year-old), young *ATF4*$^{-/-}$(3-months-old) and *ATF4*$^{-/-}$(1-year-old) donor BM-derived cells in recipient PB at 8 weeks after competitive BMT (n=5-8 mice per group).

(D) The bar graphs display the percentages of *ATF4*$^{-/-}$ (3-months-old), *ATF4*$^{-/-}$ (1-year-old) and their corresponding competitor donor BM-derived T, B and myeloid cells of the recipient mice at 8 weeks after BMT (n=5-8 mice per group). Young *ATF4*$^{-/-}$ group: recipients reconstituted with young *ATF4*$^{-/-}$ BM cells and competitors, Old *ATF4*$^{-/-}$ group: recipients reconstituted with old *ATF4*$^{-/-}$ BM cells (1-year-old) and competitors.

Note: The figures based on Figure 4E, 4O, 4F and 4P, directly comparing young with aged *ATF4* KO group.

*P<0.05, **P<0.01 and $^{\#}P$<0.001 (t test).

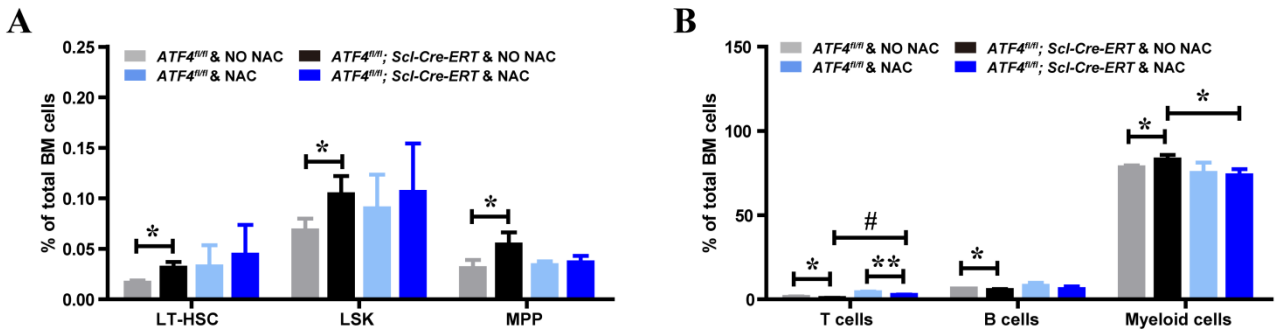

fig. S5. Mitochondrial ROS contributes to ATF4 deficiency induced HSC defects.

(A, B) The frequency of LT-HSCs, MPP, and LSK cells (**A**) (n=3-4 mice per group), and T, B and myeloid cells (**B**) (n=2-4 mice per group) in BM cells from tamoxifen-induced *ATF4*$^{fl/fl}$ and *ATF4*$^{fl/fl}$; *Scl-Cre-ERT* mice with or without NAC administration.

Note: The figures based on Figure 3H, 3I, 5H and 5I, directly comparing NAC with NO NAC treated group.

*P<0.05, **P<0.01 and $^{\#}P$<0.001 (t test).

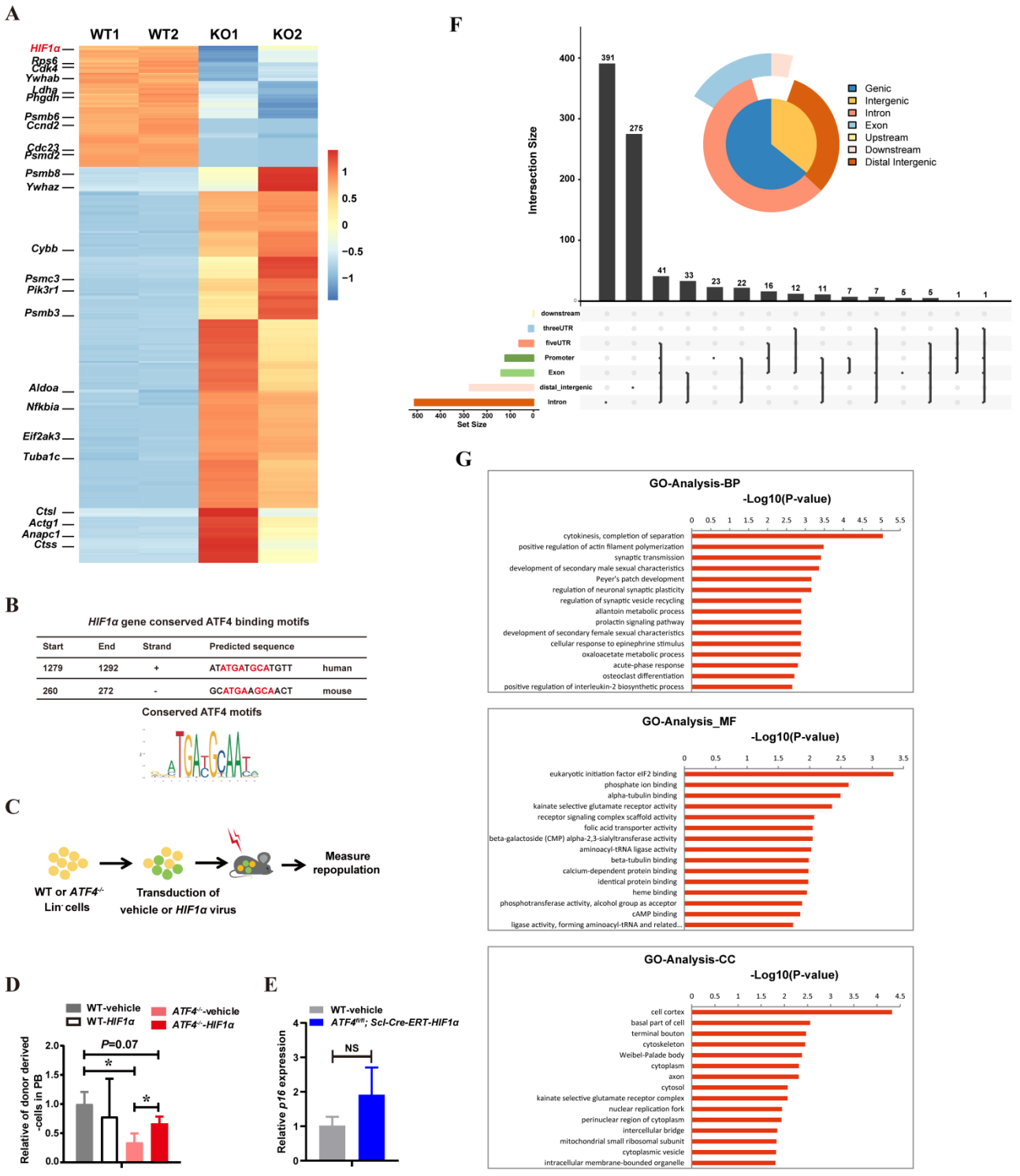

fig. S6. ATF4 deficiency-induced HIF1α downregulation involved in the HSC impairment and AML development..

(A) Heat map of RNA-seq analysis of differentially expressed genes in WT and *ATF4*$^{-/-}$ LT-HSCs.

(B) Identified ATF4 consensus-binding motifs in the promoter of the *HIF1α* gene.

(C) Schematic design of rescuing experiment on *HIF1α* overexpression in WT and *ATF4*$^{-/-}$ Lin^{-} cells.

(D) Repopulation analysis of donor-derived PB chimeras of WT or *ATF4*$^{-/-}$ donor cells transduced with recombinant retrovirus carrying *HIF1α* after BMT (n=3 mice per group).

(E) mRNA expression of *p16*^{Ink4a} in control and *ATF4*$^{fl/fl}$*; Scl-Cre-ERT* donor-derived BMCs after HIF1α rescue.

(F, G) ChIP-seq assay reveal genomic distribution of sequence peaks captured by the antibodies compared with the whole genome of KG1α cells (**F**) and GO enrichment with top-ranked classification (P< 0.05) (**G**).

**P*<0.05, ***P*<0.01 and $^{\#}$*P*<0.001 (t test).